Physics Letters B 807 (2020) 135610

Contents lists available at ScienceDirect

Physics Letters B

www.elsevier.com/locate/physletb

Acceleration induced neutron emission in heavy nuclei

N. Carjan [a,b,*], M. Rizea [a]

[a] National Institute for Physics and Nuclear Engineering "Horia Hulubei", Str. Reactorului no. 30, P.O. BOX MG-6, Bucharest - Magurele, Romania
[b] CENBG, University of Bordeaux, 33175 Gradignan, France

ARTICLE INFO

Article history:
Received 12 March 2020
Received in revised form 1 July 2020
Accepted 6 July 2020
Available online 10 July 2020
Editor: J.-P. Blaizot

Keywords:
Neutron emission
Acceleration
Moving potential
Time-dependent Schrödinger equation

ABSTRACT

The effect of the acceleration of a nucleus on the neutron states is studied in the frame of the independent-particle nuclear shell model. For this we solve numerically the time-dependent Schrodinger equation, with a moving mean-field of Woods-Saxon type. The time evolution of a neutron states at the Fermi level is calculated for ^{236}U and acceleration parameter A=0.5 (in 10^{44} [fm/sec^2]). It is the acceleration during the Coulomb repulsion of two ^{236}U nuclei when they are 20 fm apart. We keep this acceleration constant for 10^{-21} sec before we switch it off (A=0) and follow the wave packet for another 10^{-21} sec. During the acceleration, the wave function oscillates with increasing amplitude until it escapes, mainly in the direction opposite to the motion of the nucleus. The mean value of its energy (in the nuclear system) increases from −4.80 MeV to −3.15 MeV and 12% of the wave packet leaves the nucleus. During the uniform motion, the wave packet continues to oscillate and to escape at a lower rate: an extra 2%. We repeated the calculations for two neighboring states and found the emission rate to depend strongly on the position of the neutron state with respect to the Fermi energy. Finally, the effect of the nuclear deformation on the acceleration induced neutron emission is studied. In this case the period of oscillation is larger and the amplitude smaller. The angular distribution with respect to the direction of motion is more complex: it has, in the nuclear system, an intense component almost perpendicular to the deformation axis.

What if, like a fully-filled water tank, a nucleus will spill its less bound nucleons when accelerated? Most probable this could happen to neutrons since, contrary to protons, they are not protected by a Coulomb barrier. In case the answer is "yes", we are dealing with a new way of neutron emission from nuclei.

Acceleration of heavy nuclei is an integral part of nuclear fission and reactions induced by heavy-ions. If neutrons are emitted during the acceleration of the fission fragments or when the projectile moves closer to or away from the target, one has to take into account this emission in the analysis of the data.

To give a first answer to this captivating question we choose a simple framework: the independent particle shell model [1] and a simple scenario borrowed from the operating mode of a linear accelerator [2]. We therefore solve the time-dependent Schrödinger equation with a moving mean-field of Woods-Saxon type and study the change in the neutron eigenstates during 10^{-21} sec of constant acceleration followed by 10^{-21} sec of constant velocity.

As in the independent particle shell model, we look at one neutron at a time. It moves in a mean field created by all other nucleons. At the same time it contributes to the potential seen by the others. If the nucleons are displaced, the nuclear density is displaced and, by selfconsistency, the potential follows. As for the shell model, our approach is expected to work for weakly bound nucleons.

The motion of a quantum particle in a moving one-dimensional potential well has been already studied in the field of control systems [3–5].

In our case, we consider a neutron in a moving nuclear potential that has axial symmetry. It is represented by a wave function solution of the Schrödinger equation

$$i\hbar\frac{\partial\Theta(\rho,z,t)}{\partial t}=\mathcal{H}(\rho,z,t)\Theta(\rho,z,t), \tag{1}$$

where $\mathcal{H}$ is the single-particle Hamiltonian.

$$\mathcal{H}=-\frac{\hbar^2}{2m}\left[\frac{1}{\rho}\frac{\partial}{\partial\rho}+\frac{\partial^2}{\partial\rho^2}+\frac{\partial^2}{\partial z^2}-\frac{\Lambda^2}{\rho^2}\right]+V(\rho,z-\alpha(t)).$$

To cover nuclei from spherical to strongly deformed, the formalism is developed in cylindrical coordinates. $\alpha(t)$ describes the displacement of the potential in time along the z axis. Λ is the projection of the orbital angular momentum on the symmetry axis. For simplicity the spin-orbit term is neglected.

* Corresponding author.
E-mail address: carjan@in2p3.fr (N. Carjan).

https://doi.org/10.1016/j.physletb.2020.135610

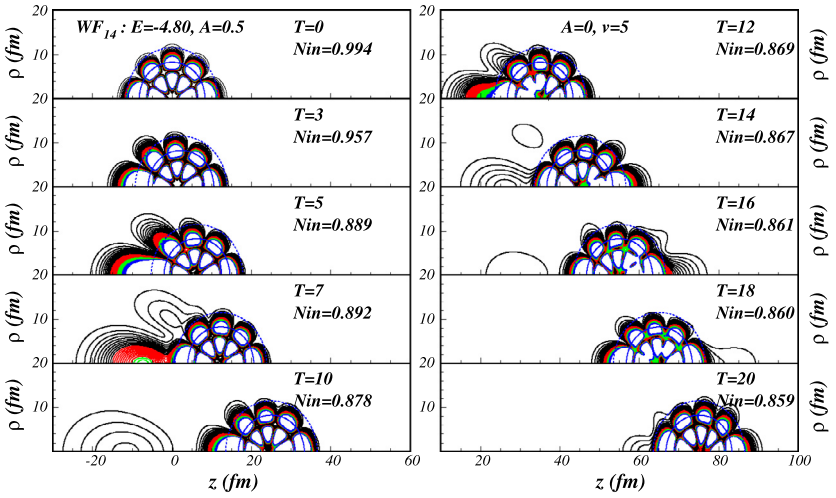

Fig. 1. Time evolution of $|\Phi^0_{14}|^2$ during (left) and after (right) acceleration for spherical ^{236}U. N_{in} is the norm inside the dotted circle defined by $V_0/100$. T is the time in 10^{-22} sec.

By the Liouville transformation $\Phi = \rho^{1/2}\Theta$, the first derivative with respect to ρ from $\mathcal{H}$ is removed, resulting a simplified Hamiltonian H of the form:

$$H = -\frac{\hbar^2}{2m}\left[\frac{\partial^2}{\partial\rho^2} + \frac{\partial^2}{\partial z^2} - \frac{\Lambda^2 - 1/4}{\rho^2}\right] + V(\rho, z - \alpha(t)).$$

To solve the corresponding equation, a transformation of both the variable and the function from the non-inertial (laboratory) to the inertial (nuclear) system is convenient. It avoids an interpolation of the potential between the grid points at each time step.

We will explain this transformation on the 1-D TDSE:

$$i\hbar\frac{\partial\Phi(t,z)}{\partial t} = -\frac{\hbar^2}{2m}\frac{\partial^2\Phi(t,z)}{\partial z^2} + V(z-\alpha(t))\Phi(t,z) \tag{2}$$

We go in the nuclear frame by the following changes of the variable $z \to q$ and of the function $\Phi \to \Psi$ [6]:

$$q = z - \alpha(t), \quad \Phi(t,z) = \exp(u)\Psi(t,q) \tag{3}$$

where

$$u = ib\left(z\dot{\alpha} - \alpha\dot{\alpha} + \frac{1}{2}\int_0^t \dot{\alpha}^2(t')dt'\right).$$

By taking $b = \frac{m}{\hbar}$, it can be shown that Eq.(2) will be transformed in

$$i\hbar\frac{\partial\Psi(t,q)}{\partial t} = -\frac{\hbar^2}{2m}\frac{\partial^2\Psi(t,q)}{\partial q^2} + V(q)\Psi(t,q) + mq\ddot{\alpha}(t)\Psi(t,q). \tag{4}$$

To eliminate the linear term in q (which tends to ∞ as $q \to \infty$), a further function transformation is performed [7]

$$\Psi(t,q) = \exp\left(-i\frac{\lambda}{\hbar}\right)\chi(t,q) \tag{5}$$

with

$$\lambda(t,q) = qm\int_0^t \ddot{\alpha}(t')dt' = q\beta(t).$$

In our particular case $\alpha(t) = \frac{1}{2}At^2$.

$\dot{\alpha} = At, \ddot{\alpha} = A, \lambda = Bqt, B = mA$

$$u = ib\left(zAt - \frac{1}{3}A^2t^3\right)$$

and the equation for χ assumes the form:

$$i\hbar\frac{\partial\chi(t,q)}{\partial t} = -\frac{\hbar^2}{2m}\left(\frac{\partial^2\chi(t,q)}{\partial q^2} + \frac{2}{\hbar i}Bt\frac{\partial\chi(t,q)}{\partial q} - \frac{1}{\hbar^2}B^2t^2\chi(t,q)\right) + V(q)\chi(t,q). \tag{6}$$

The advantage of these transformations is that they lead to equations in which the potential depends on a time-independent variable, the dependence on $\alpha(t)$ being transferred in the coefficients of Eqs. (4), (6).

Since the potential moves along the z-axis, the inclusion of the second coordinate ρ is straightforward. We therefore work with the variables ρ and q on a finite numerical grid: $[0, 160]$x$[-256, 256]$, $\Delta\rho = \Delta q = 1/8$ fm. For the time evolution we use the step $\Delta t = 1/128 \times 10^{-22}$ sec. The equations (4) and (6) are solved numerically by the Crank-Nicolson method. One obtains a linear system which is solved by a routine based on the Strong Implicit Procedure [8]. As initial solutions (at $t = 0$) we consider eigenfunctions of the original Hamiltonian.

The propagation in time is done in two steps. We consider a quadratic α(t) and use Eq. (6) for 10^{-21} sec. Then we consider a linear α(t) and use Eq. (4) without the $\ddot{\alpha}$ term for another 10^{-21} sec. At any time, by performing the inverse tranformations, we can retrieve the solution $\Phi(\rho, z, t)$ of the original equation. For the 1st step we choose the constant acceleration A=0.5[10^{44} fm/sec^2] resulting a constant velocity $v = 5[10^{22}$ fm/sec$] = 0.167$c for the 2nd step. c is the speed of light. As first example, we take spherical ^{236}U and study 3 neutron states with $\Lambda = 0$ around the Fermi level. The parameters of the Woods-Saxon potential are fitted to single-particle and single-hole states in the ^{208}Pb region [9].

Fig. 1 shows the result for the 14th eigenstate laying at -4.8 MeV. For T $>$ 0, the wave packet exhibits a changing asymmetry with respect to the ρ axis indicative of an oscillation. In fact, we are dealing with an oscillation over the usual vibration of a quasi-stationary state. A similar vibration causes the barrier assaults in the Gamow picture of α decay [10]. The presence of the neutron inside the nucleus, measured by N_{in}, decreases from 1.00 (at T=0) to 0.88 (at T=10). A neutron, initially occupying this state, has therefore 12% chance to be emitted during the acceleration phase. For T $>$ 10 the oscillatory motion continues. At T=20 N_{in} reaches

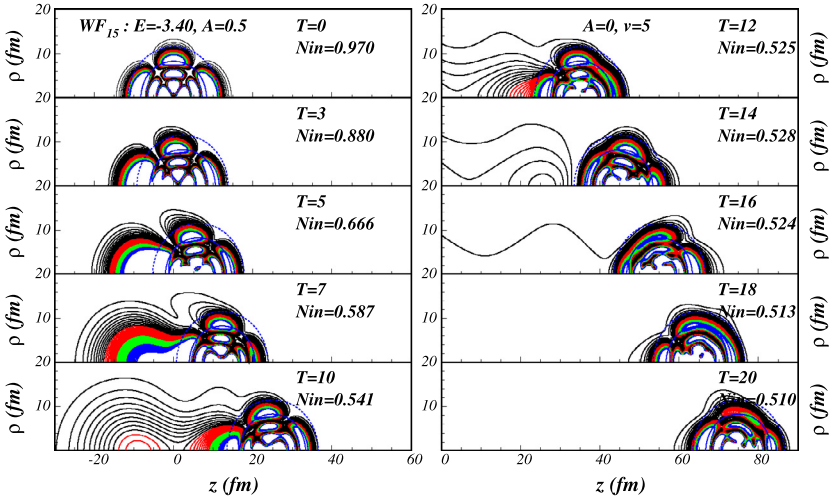

Fig. 2. The same as in Fig. 1 but for Φ^0_{15}.

an even lower value (0.86) because at T=10 the wave packet has short unbound tails which will inevitably leave the nucleus.

The most probable direction of emission is 180° with respect to the displacement of the nucleus as in classical mechanics. There is however a weaker branch at ≈150° which has a quantum origin. It is known that the tunneling path of a metastable state is mainly dictated by its quantum numbers [11,12]. In other words the emission preserves the spatial distribution of the respective state. Hence we expect a 2nd peak at 125° in the nuclear system which translates into an emission at 150° in the laboratory system.

Fig. 2 shows the time dependence of a neutron states with energy (−3.4 MeV) above the Fermi level. 49% of this wave function is emitted, in the same interval of time, through strong oscillations. Predictably, the emission starts earlier and is more intense. As for Φ^0_{14}, there are also two directions of emission: one intense at 180° and one weak at an angle between 180° and 90°.

A wave function with energy lower than the Fermi level was found to oscillate during both regimes: quadratic and linear $\alpha(t)$. It doesn't however succeed to escape: its presence inside the nucleus doesn't change.

The percentage of the wave packet that leaves the nucleus, $N_{in}(0) - N_{in}(T)$, is a measure of the neutron emission probability. We have plotted this quantity as a function of time for Φ^0_{14} and Φ^0_{15} in Fig. 3. As expected, neutrons that are less bound have higher emission probability. One can observe the effect of the oscillation of the wave function in the mean-field and the plateau at large times (the emission is gradually reduced when the acceleration is turned off).

Summing up, we start with an eigenstate that, due to acceleration, becomes wave packet, i.e., it occupies with time dependent probabilities neighboring states (oscillation) including some in the continuum (emission).

For a better understanding of the physics involved, we divide the total energy in the laboratory system in significant terms:

$$\begin{aligned}\langle\Phi|H|\Phi\rangle = &-\frac{\hbar^2}{2m}\iint\left(\Psi^*\frac{\partial^2\Psi}{\partial\rho^2}+\Psi^*\frac{\partial^2\Psi}{\partial q^2}\right)d\rho dq\\ &+\frac{\hbar^2}{2m}b^2\dot{\alpha}^2\iint|\Psi|^2d\rho dq-\frac{\hbar^2}{2m}2ib\dot{\alpha}\iint\Psi^*\frac{\partial\Psi}{\partial q}d\rho dq\\ &+\frac{\hbar^2}{2m}\left(\Lambda^2-1/4\right)\iint\frac{1}{\rho^2}|\Psi|^2d\rho dq\\ &+\iint V(\rho,q)|\Psi|^2d\rho dq. \qquad (7)\end{aligned}$$

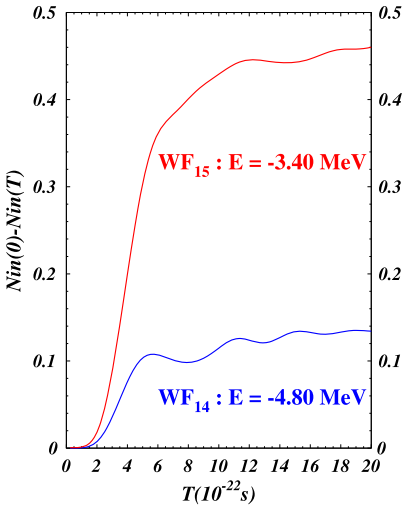

Fig. 3. The neutron emission probability as a function of time for Φ^0_{14} and Φ^0_{15}.

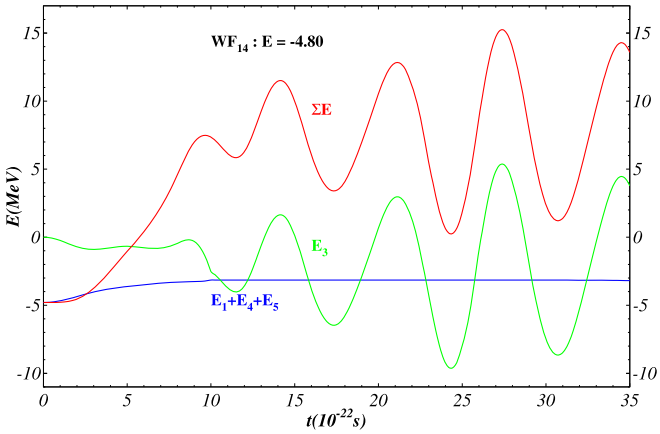

Fig. 4. The neutron energy in the laboratory system (red), in the nuclear system (blue) and the energy due to the interaction with the moving potential (green).

The 1st term is the average kinetic energy in the nuclear frame. The 2nd term reduces to $m\dot{\alpha}^2/2$; it is the extra kinetic energy due to the velocity of the potential. The 3rd term reduces to $\dot{\alpha} < p >$ where $< p >$ is the average momentum in the nuclear frame. It represents the variation of the neutron energy due to the inter-

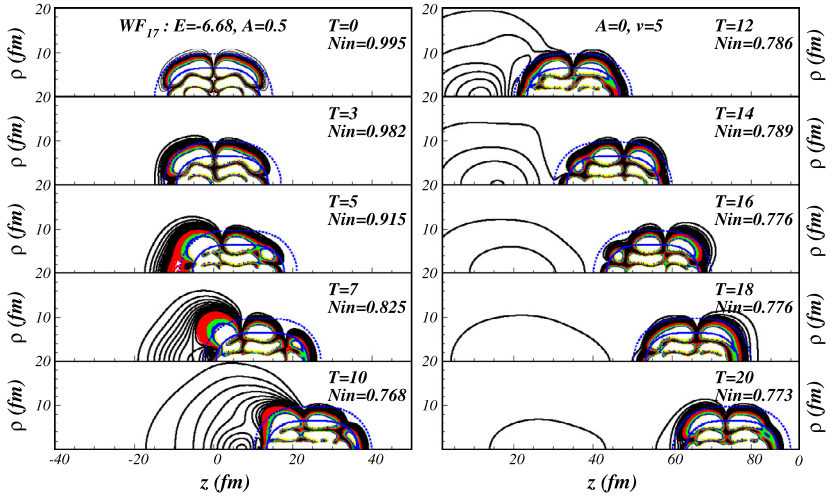

Fig. 5. Time evolution of $|\Phi^0_{17}|^2$ during (left) and after (right) acceleration for the shape isomer (deformation parameter $\epsilon = 0.52$) of ^{236}U. N_{in} is the norm inside the dotted ellipse defined by $V_0/100$. T is the time in 10^{-22} sec.

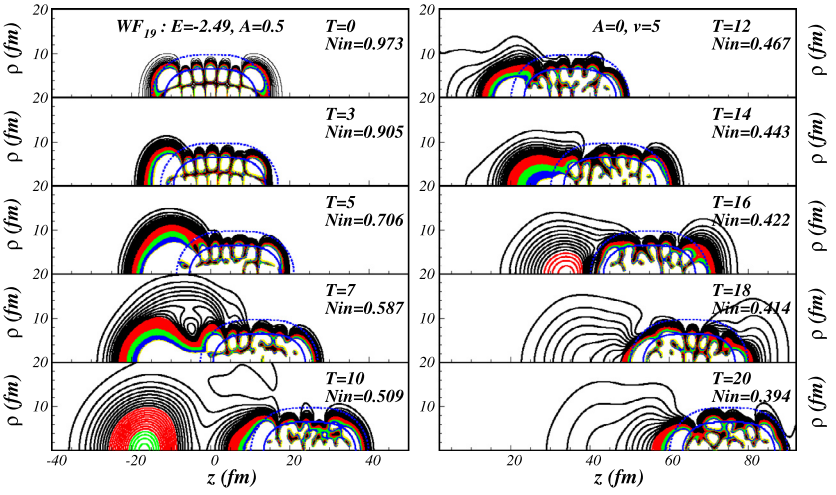

Fig. 6. The same as in Fig. 5 but for $|\Phi^0_{19}|^2$.

action with the moving wall of the potential; equivalent to the "one-body" dissipation [13]. The last two terms are the average centrifugal and nuclear potentials respectively.

The sum E1+E4+E5 i.e., the average neutron energy in the nuclear frame, slightly increases up to T=10 and stays constant afterwards. After T=10 the oscillations of E are due only to E3 as clearly seen in Fig. 4.

In the absence of correlations the oscillations last long time. In reality, with increasing excitation energy, the time between collisions decreases and the oscillations are slowly damped due to the onset of correlations.

Finally we study the effect of nuclear deformation on the neutron emission due to acceleration of the nucleus along the deformation axis. For this we describe the nuclear shape by a pure Cassini oval with a prolate deformation parameter $\epsilon = 0.52$. It represents the shape isomer of ^{236}U [14]. The results for two neutron states, one below and one above the Fermi level, are presented in Figs. 5 and 6 respectively. The emission probability is again larger in the latter case: $N_{in} = 0.77$ vs 0.39. One can also notice that the emission at angles smaller than 180° to the z-axis is much intenser than in the previous cases. It is because a quasi-stationary state in a deformed nucleus tunnels most probably pependicularly to the deformation axis [15], irrespective if the barrier is lower or higher along this direction. It is what happens here: the emission occurs at 90° in the nuclear system. Due to the displacement of the nucleus however, in the laboratory system, the emission occurs at slightly larger angles (≈110°). Hence there is a qualitative difference between spherical and strongly deformed nuclei: in the latter case, the direction imposed by quantum mechanics competes in intensity with the classically expected direction of emission.

Since in the present calculation the potential moves in the z-direction (Eq. (2)), one can study nuclei with the deformation axes aligned with the velocity vector (axial symmetry). In heavy-ion reactions however a deformed projectile approaches a target with different orientations of the deformation axes. For a quantitative evaluation, an average over all orientations has to be performed.

This type of neutron emission doesn't occur only during the acceleration of a nucleus but also during the slowing down (A<0) of a projectile when it approaches a target. Among possible effects, an increase of the neutron-transfer cross section is expected.

The chosen value of A (0.5) is two times larger than the acceleration during the Coulomb repulsion of two equal fission fragments from ^{236}U separated by $D_{cm} = 20$ fm (A=0.249) but comparable with that for the collision of two ^{236}U nuclei at the same distance of approach (A=0.498). In conclusion, the excitation of the fission fragments during their acceleration (separation) is improbable. On the other hand, a heavy projectile could become excited (even emit neutrons) when it approaches a heavy target or moves away

from it. For a quantitative answer a dedicated study is necessary. The acceleration produced in Coulomb interactions is not constant, it depends on $D_{\rm cm}$. A high level can be however maintained for 10^{-21} sec, a short time at the scale of the above mentioned processes (10^{-20} sec).

A heavy-ion of mass m and charge q in an electric field E is accelerated along the field lines; $a = qE/m = 0.376 \times 10^{23} \times E[\mathrm{fm/s^2}]$ with E in [V/m]. To attain an acceleration comparable with the one used above requires $E = 10^{21}$ [V/m] i.e., a much too large value.

A comment on the peculiarity of accelerating a heavy-ion is appropriate. Altough all forces that produce the acceleration of heavy ions (such as the Coulomb force or the force qE exerted by an electric field E on a charge q) act only on protons, the neutrons follow. To decouple the two fields one needs extreme conditions. For instance to excite an isovector giant dipole resonance, a relativistic projectile is necessary [16].

The process of acceleration induced neutron emission has similarities with the realease of neutrons at scission i.e., during the last stage of nuclear fission [17,18]. They are both due to a fast change of the potential in which they move that transforms each neutron state into a wave packet with components in the continuum. In the case of scission neutrons however, it is the shape of the potential and not its position that changes.

A more quantitative evaluation of this process requires a time-dependent, self-consistent microscopic approach [19]. At present it is a difficult task considering the large numerical grid that is necessary.

We are grateful to Walter Furman, Gurgen Ter-Akopian and Jorgen Randrup for their interest in this work and illuminating discussions.

Declaration of competing interest

The authors declare that they have no known competing financial interests or personal relationships that could have appeared to influence the work reported in this paper.

References

[1] M. Goeppert-Mayer, J.H.D. Jensen, Nuclear Shell Structure, John Wiley and Sons, New York, 1955.
[2] H. Wiedemann, Particle Accelerator Physics, Springer, Berlin, 1999.
[3] P. Rouchon, Control of a quantum particle in a moving potential well, in: Proceedings of the 2nd IFAC Workshop on Lagrangian and Hamilton Methods for Nonlinear Control, Seville, 2003, p. 317.
[4] K. Beauchard, J.-M. Coron, Controllability of a quantum particle in a moving potential well, J. Funct. Anal. 232 (2006) 328.
[5] S. Miyashita, Conveyance of a quantum particle by a moving potential well, J. Phys. Soc. Jpn. 76 (2007) 104003.
[6] A.G. Butkovsky, Y.I. Samoilenko, Control of Quantum- Mechanical Processes and Systems, Mathematics and Its Applications (Soviet Series), vol. 56, Kluver Academic Publishers, Dortrecht/Boston/London, 1990, English edition.
[7] C-C. Chou, R.E. Wyatt, Time-dependent Schrodinger equation with Markovian outgoing wave boundary conditions: applications to quantum tunneling dynamics and photoionization, Int. J. Quant. Chem. 1 (13) (2013) 39.
[8] C.R. Jesshope, SIPSOL - suite of subprograms for the solution of the linear equations arising from elliptic partial differential equations, Comput. Phys. Commun. 1 (7) (1979) 383.
[9] E. Rost, Proton shell-model potential for lead and the stability of superheavy nuclei, Phys. Lett. B 26 (1968) 184.
[10] S.A. Gurwitz, G. Kalberman, Decay width and shift of a quasistationary state, Phys. Rev. Lett. 59 (1987) 262.
[11] P. Talou, N. Carjan, D. Strottman, Time-dependent approach to bidimensional quantum tunneling: application to the proton emission from deformed nuclei, Nucl. Phys. A 647 (1999) 21.
[12] N. Carjan, P. Talou, D. Strottman, Angular distribution of protons emitted from oriented nuclei: toward imaging single-particle wave functions, in: Smit, et al. (Eds.), The Nucleus: New Physics for the New Millenium, Kluver Academic/Plenum Publishers, New York, 2000, p. 115.
[13] J. Blocki, Y. Boneh, J.R. Nix, M. Robel, A.J. Sierk, W.J. Swiatecki, One-body dissipation and the super-viscidity of nuclei, Ann. Phys. 113 (1978) 330.
[14] V. Pashkevich, On the asymmetric deformation of fissioning nuclei, Nucl. Phys. A 169 (1971) 275.
[15] D. Strottman, N. Carjan, P. Talou, New aspects in the decay of quasi-stationary states by multidimensional tunneling, Phys. Scr. T 88 (2000) 148.
[16] I. Stetcu, C.A. Bertulani, A. Bulgac, P. Magierski, K.J. Roche, Relativistic Coulomb excitation within the time dependent superfluid local density approximation, Phys. Rev. Lett. 114 (2015) 012701.
[17] M. Rizea, N. Carjan, Dynamical scission model, Nucl. Phys. A 909 (2013) 50.
[18] N. Carjan, M. Rizea, Similarities between calculated scission-neutron properties and experimental data on prompt fission neutrons, Phys. Lett. B 747 (2015) 178.
[19] C. Simenel, A.S. Umar, Heavy-ion collisions and fission dynamics with the time-dependent Hartree-Fock theory and its extensions, Prog. Part. Nucl. Phys. 103 (2018) 19.